pH-Independent, 520 mV Open-Circuit Voltages of Si/Methyl Viologen$^{2+/+}$ Contacts Through Use of Radial n$^+$p-Si Junction Microwire Array Photoelectrodes

Emily L. Warren, Shannon W. Boettcher,[⊥] Michael G. Walter, Harry A. Atwater,* and Nathan S. Lewis*

Division of Chemistry and Chemical Engineering, Division of Engineering and Applied Science, Kavli Nanoscience Institute and Beckman Institute, 210 Noyes Laboratory 127-72, California Institute of Technology, Pasadena, California 91125, United States

Received: September 24, 2010; Revised Manuscript Received: November 26, 2010

The effects of introducing an n$^+$-doped emitter layer have been evaluated for both planar Si photoelectrodes and for radial junction Si microwire-array photoelectrodes. In contact with the pH-independent, one-electron, outer-sphere, methyl viologen redox system (denoted $MV^{2+/+}$), both planar and wire array p-Si photoelectrodes yielded open-circuit voltages, V_{oc}, that varied with the pH of the solution. The highest V_{oc} values were obtained at pH = 2.9, with $V_{oc} = 0.53$ V for planar p-Si electrodes and $V_{oc} = 0.42$ V for vapor−liquid−solid catalyzed p-Si microwire array samples, under 60 mW cm^{-2} of 808 nm illumination. Increases in the pH of the electrolyte produced a decrease in V_{oc} by approximately −44 mV/pH unit for planar electrodes, with similar trends observed for the Si microwire array electrodes. In contrast, introduction of a highly doped, n$^+$ emitter layer produced $V_{oc} = 0.56$ V for planar Si electrodes and $V_{oc} = 0.52$ V for Si microwire array electrodes, with the photoelectrode properties in each system being essentially independent of pH over six pH units ($3 < pH < 9$). Hence, formation of an n$^+$ emitter layer not only produced nearly identical photovoltages for planar and Si microwire array photoelectrodes, but decoupled the band energetics of the semiconductor (and hence the obtainable photovoltage) from the value of the redox potential of the solution. The formation of radial junctions on Si microwire arrays thus provides an approach to obtaining Si-based photoelectrodes with high-photovoltages that can be used for a variety of photoelectrochemical processes, including potentially the hydrogen evolution reaction, under various pH conditions, regardless of the intrinsic barrier height and flat-band properties of the Si/liquid contact.

I. Introduction

P-type silicon is a promising material for the H_2-producing photocathode of a dual photosystem water-splitting device, because p-Si has a bandgap (1.1 eV) that is thermodynamically ideal for an optimized dual bandgap solar water-splitting system,[1] the band edges of Si span the H^+/H_2 redox potential, and p-Si is purportedly stable in water under cathodic conditions. However, due to its indirect bandgap, and thus long optical absorption depth (∼200 μm), efficient planar Si-based devices require the use of high-purity Si.

In contrast to the planar structure, a radial wire array architecture decouples the directions of light absorption and charge carrier diffusion, enabling the use of Si with shorter minority-carrier diffusion lengths than would be acceptable in a planar geometry.[2] Arrays of Si microwires grown by the vapor−liquid−solid (VLS) process have shown promising performance in regenerative photoelectrochemical cells and in photovoltaic devices.[3,4] Specifically, p-Si microwire arrays grown from Cu VLS catalysts exhibit internal quantum yields for carrier collection that approach unity, and open-circuit voltages (V_{oc}) of up to 0.45 V, in contact with the aqueous methyl viologen redox system ($MV^{2+/+}$).[3,5] Solid-state radial n$^+$p junction microwire arrays have yielded photovoltages >500 mV under Air Mass 1.5 simulated illumination.[4] For solar-fuel-generating applications, these wire arrays are also interesting because the wires can be embedded in a flexible polymer,[6] and the enhanced surface area of the wire array relative to a traditional planar geometry allows for the facile integration of fuel-forming catalysts to efficiently affect chemical processes such as the hydrogen evolution reaction (HER).[6,7]

P-type Si electrodes, however, yield significantly smaller photovoltages in contact with the H^+/H_2 redox system than the >500 mV photovoltages achievable in contact with redox species such as $MV^{2+/+}$ (aq).[8,9] The valence band-edge potential of Si is only ∼300 mV more positive than the H^+/H_2 formal reduction potential, limiting the built-in voltage at such semiconductor/liquid contacts. This low photovoltage thus limits the application of p-Si in an overall water-splitting device, in which a total photovoltage of >1.23 V must be generated. The potential of the H^+/H_2 redox couple, $E(H^+/H_2)$, can be manipulated relative to a fixed reference potential by changing the pH of the solution, but the band-edge positions of Si in H_2O are also sensitive to pH, resulting in a nearly constant photovoltage as the pH of the contacting solution is varied.[10]

If the band-edge positions of the Si could be controlled to eliminate the dependence on pH, the photovoltage of p-Si/H^+/H_2(aq) contacts could be increased by simply increasing the pH of the aqueous electrolyte. Functionalization of n-Si surfaces with methyl groups, through two-step chlorination/alkylation chemistry, has been shown to largely eliminate the pH dependence of planar Si electrodes.[11] However, the surface-dipole produced by methyl termination shifts the Si band edges toward the vacuum level, decreasing the attainable photovoltage in a

* To whom correspondence should be addressed. E-mail: haa@caltech.edu (H.A.A); nslewis@caltech.edu (N.S.L.).
[⊥] Current Address: Dept. of Chemistry, University of Oregon.

10.1021/jp109147p
Published on Web 12/23/2010

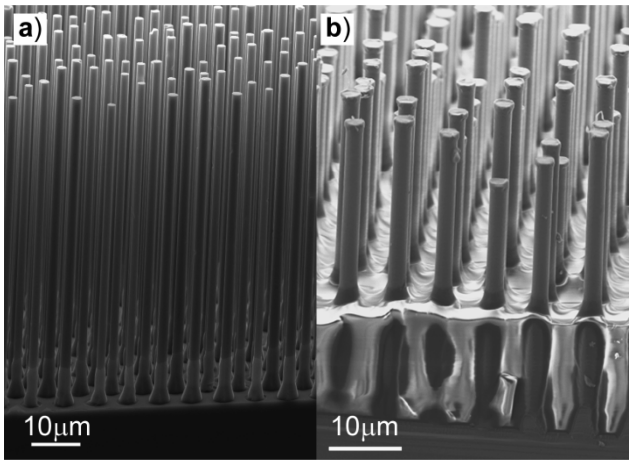

Figure 1. (a) SEM image of p-Si wires with an oxide boot at the base of the wires and (b) of a diffused n^+p-Si wire array infilled with mounting wax (to prevent shunting).

photocathode.[11−13] Another approach would involve formation of a p−n homojunction in the Si, to thereby physically separate the rectifying junction from the liquid contact and from any surface-attached catalysts. Consistently, planar p−n Si junctions[14] and microparticulate crystalline Si homojunction systems[15] have been reported to exhibit increased photovoltages in contact with an electrolyte, relative to the analogous Si/liquid contacts.

In this work, we have investigated the pH dependence of the photoelectrode behavior of VLS-grown Si microwire photocathodes (and planar p-Si controls) with and without radial diffused n^+p junctions. Methyl viologen ($MV^{2+/+}$) is a water-stable, single-electron, outer-sphere redox couple whose reduction potential is independent of pH.[11] The energetics of the direct p-Si/$MV^{2+/+}$ contact should change as a function of pH, due to the well-known dependence of the flat-band potential of Si on the pH of the solution. In contrast, introduction of an n^+-doped emitter layer, to create a "buried junction", should decouple the band banding, and thus the photovoltage, of the photoelectrode from the energetics of the semiconductor/liquid contact. The ability to decouple the photovoltage of a Si photocathode from the pH of the contacting aqueous solution should increase the versatility of these materials for use in photoelectrochemical fuel-forming systems.

II. Experimental Methods

A. Materials. All chemicals were used as received. Water was obtained from a Barnstead Nanopure system and had a resistivity of 18.3 MΩ·cm. Planar n^+p-Si samples were fabricated from boron doped p-Si (100)-oriented, $\rho = 0.1$ Ω·cm resistivity wafers (Silicon Inc.). Planar p-Si samples were fabricated from boron doped p-Si (100)-oriented, $\rho = 0.7$ Ω·cm wafers (Silicon, Inc.). VLS-catalyzed Si wire arrays were grown on degenerately doped p-Si (111)-oriented substrates with $\rho =$ 0.003 Ω-cm (Silicon Quest International).

B. VLS Wire Growth. Si microwire arrays were grown from $SiCl_4$ using thermally evaporated Cu (6N, EPSI) as the VLS growth catalyst, and were doped p-type by the introduction of BCl_3 during growth (see Supporting Information).[3,16] The resulting wires were 2.0−2.5 μm in diameter and 50−70 μm in length (Figure 1a). The VLS catalyst tips were removed by etching the samples in buffered hydrofluoric acid (BHF; Transene, Inc.) for 10 s, followed by 5:1:1 H_2O:HCl:H_2O_2 (by volume) at 70 °C (RCA 2) for 20 min. The outer surface of the wires was etched using 4.5 M KOH (Fluka 99.995%) for 30 s at room temperature, followed by a 10 s etch in BHF. An ∼200 nm-thick dry thermal oxide was then grown on the wires by exposure to a flow of ultrahigh purity O_2 at 1100 °C for 2 h. A solution of 4.4 g of hexamethylcyclotrisiloxane (Sigma-Aldrich) (HMCTS), 1 g of polydimethylsiloxane (PDMS; Sylgard 184, Dow Corning), 0.10 g of PDMS curing agent, and 6.5 g of CH_2Cl_2 were drop-cast onto the wire array and spun at 1000 rpm for 30 s. The samples were cured on a hot plate at 150 °C for 30 min, which allowed the HMCTS to evaporate, leaving a thin (5−15 μm) layer of PDMS at the base of the wires.[6]

To etch the thermal oxide layer off of the tops of the wires, the array was rinsed with a 1:1 mixture of 1.0 M tetra(*n*-butyl) ammonium fluoride (TBAF) in tetrahydrofuran (Sigma-Aldrich) and dimethylformamide (DMF) (referred to as "PDMS etch"), rinsed with H_2O, and then etched in BHF for 5 min. The PDMS etch-barrier was removed by etching the sample in PDMS etch for 30 min. These wire arrays that contained oxide "boots" (Figure 1a) provided a direct comparison to the wire arrays that had radial n^+p junctions, because both types of arrays were fabricated with nominally identical processes to this point and had the same active junction area. The doping density of the wires was 2×10^{17} cm^{-3}, as determined by four-point probe measurements on single microwires.[17,18]

C. Fabrication of n^+p Junctions. ***1. Planar.*** Prior to diffusion of the n^+ emitter, boron-doped p-Si, $\rho \sim 0.1$ Ω·cm wafers were cleaved into 3 cm × 3 cm chips and cleaned using an RCA etch: (15 min 6:1:1 by volume H_2O:H_2O_2 (30% in H_2O):conc. (aq) NH_4OH at 75 °C (RCA 1), followed by 15 min in 6:1:1 by volume H_2O:H_2O_2 (30% in H_2O):conc. (aq) HCl at 75 °C (RCA 2)). The chips were then etched for 30 s in BHF, rinsed in H_2O, and dried with N_2. Samples were loaded onto a quartz boat between solid source CeP_5O_{14} diffusion wafers (Saint-Gobain, PH-900 PDS) and heated at 850 °C for 15 min under a N_2 ambient in a tube furnace. Samples were then etched in BHF for 30 s to remove the dopant glass from the surface. A back contact was made by evaporating ∼100 nm of Al onto the back surface, and then annealing the wafers at 800 °C for 10 min to drive the Al through the thin n^+ layer.[19] Spreading resistance measurements indicated that the surface concentration was $>1 \times 10^{19}$ cm^{-3} and the n^+ emitter layer was ∼200 nm thick.[20]

2. Wire Arrays. For the n^+p wire arrays, the wires were etched with BHF, rinsed with H_2O, and thoroughly dried with N_2 before loading into the diffusion furnace. The doping process was identical to that described for the planar samples. After doping, the wires were etched for 10 s in 5.8 M HF (aq). The bases of the wires were embedded in mounting wax (Quickstick 135, South Bay), to prevent shunting from any broken wires in the array. The wax was melted into the wire arrays on a hot plate at 150 °C and excess wax was removed by using a glass slide to press a KimWipe over the sample. The wax was then etched back from the tips of the wires using an O_2 plasma for ∼60 min (400 W, 300 mTorr) (Figure 1b).

D. Electrode Fabrication. Substrates were cleaved into samples of dimensions ∼0.3 cm × 0.3 cm, and the backs of the samples were scratched with a diamond scribe and dipped in BHF to expose unoxidized Si. Ga:In eutectic was then rubbed onto the backs of the Si to make ohmic contact. Samples were mounted facing downward, onto coils of tinned Cu wire that had been threaded through 7 mm diameter glass tubes. The samples were then secured to the wire using Ag paint (GC Electronics), and the wire was sealed inside the glass tube using Hysol 1C epoxy. The active area of the electrodes was defined

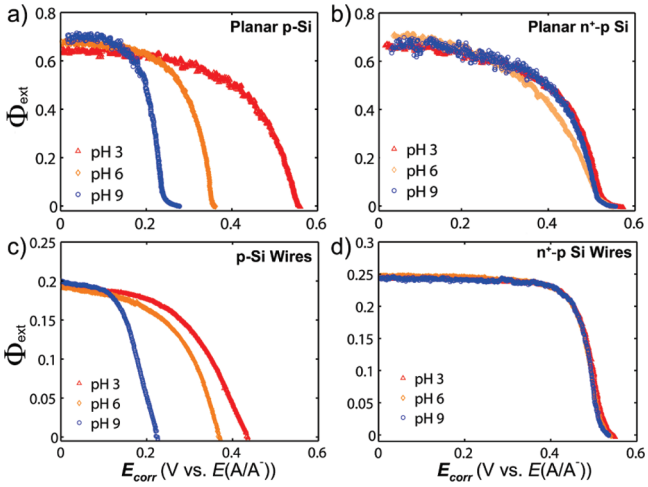

Figure 2. Representative external quantum yield (Φ_{ext}) versus potential data as a function of pH for (a) planar p-Si, (b) planar n^+p-Si, (c) p-Si wire arrays, and (d) n^+p radial junction wire arrays. Red triangles correspond to pH = 2.9, yellow diamonds to pH 5.9, and blue circles to pH 8.9. All electrodes were measured under 60 mW cm^{-2} of 808 nm illumination in aqueous solution with 50 mM $MV^{2+/+}$. Data are corrected for the solution effects, including uncompensated cell resistance (~20 Ω) and concentration overpotentials, to obtain photoelectrode performance parameters inherent to the Si electrodes (Supporting Information). Data were referenced to the solution potential, which was maintained between −0.60 and −0.59 V vs SCE by bulk electrolysis of MV^{2+} to MV^+. For samples without a diffused junction, V_{oc} decreased with increasing pH, whereas n^+p-Si samples displayed essentially no change in $\Phi_{ext}-E$ behavior, or in V_{oc}, across six pH units.

using Loctite 9460 epoxy. Electrode areas were measured with a high-resolution scanner (Epson Perfection 1200) and calculated using Image J software. Electrode areas were 0.03−0.10 cm^2.

E. Photoelectrochemical Measurements. All electrochemical measurements were carried out in a cylindrical, flat-bottomed cell equipped with four ground-glass ports. Each experiment used ~50 mL of buffer solution that contained 50 mM $MV^{2+}Cl_2$ and 0.5 M K_2SO_4(aq) as a supporting electrolyte, and was purged with Ar for 10 min prior to use. Ar continuously blanketed the cell during all experiments. The three-electrode setup consisted of a small carbon cloth reference electrode (~1 cm^2), a large carbon-cloth counter electrode (~10 cm^2), and the Si working electrode. The solution potential, $E(A/A^-)$, was kept between −0.60 and −0.59 V versus a saturated calomel electrode (SCE) by bulk electrolysis of MV^{2+} to MV^+. $E(A/A^-)$ was continuously monitored by measuring the potential at the carbon reference electrode versus an SCE in contact with the solution. The solution was continuously stirred using a magnetic stirbar placed directly adjacent to the working electrode. Each electrode was tested several times over a period of several days, to ensure that the measured performance was reproducible.

III. Results

Figure 2 shows representative external quantum yield (Φ_{ext}) versus potential (E) data for (a) planar p-Si, (b) n^+p planar Si, (c) p-Si wire array, and (d) n^+p wire array structures in contact with 47 mM MV^{2+}/3 mM MV^+ (aq) under 60 mW cm^{-2} of 808 nm illumination.[21] Each plot shows the $\Phi_{ext}-E$ data for a representative electrode in buffered solutions at pH 2.9, 5.9, and 8.9, respectively, measured versus the solution potential, $E(A/A^-)$. Si has a high kinetic overpotential for H_2 evolution, so none of the photocurrent measured is attributable to H_2

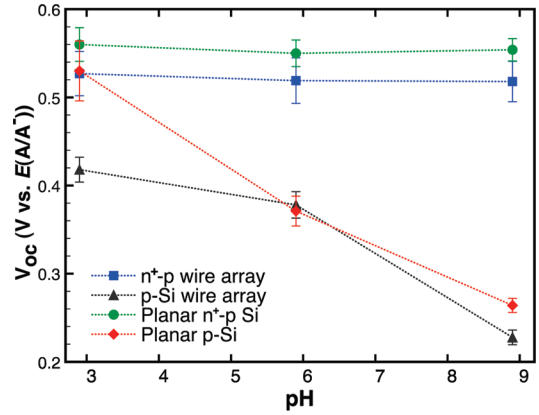

Figure 3. The dependence of V_{oc} on solution pH for radial n^+p-Si junction wire arrays, p-Si wire arrays, n^+p planar Si, and planar p-Si electrodes in contact with $MV^{2+/+}$(aq).

production in the potential range of interest.[8,22] The performance of p-Si wire array electrodes at pH 2.9 was very similar to previously reported data for Si wires that did not contain the oxide boot structure: V_{oc} = 0.42 ± 0.01 V, external quantum yield at short circuit, $\Phi_{ext,sc}$ = 0.19 ± 0.01, fill factor, ff_{808} = 0.45 ± 0.02, and an energy conversion efficiency, η_{808} = 2.3 ± 0.2%.[3] After correcting the data for concentration overpotential and uncompensated resistance losses in the cell,[23] the corrected photoelectrode fill factor and efficiency were $ff_{808,corr}$ = 0.48 ± 0.02 and $\eta_{808,corr}$ = 2.5 ± 0.2%, respectively (calculations in Supporting Information). Under the same conditions, the best performing n^+p radial junction wire array electrodes yielded V_{oc} = 0.55 V, ff_{corr} = 0.72, Φ_{ext} = 0.25 and $\eta_{808,corr}$ = 6.4%. The key energy-conversion parameters for all four types of electrodes are reported in Table S1.

Figure 3 shows the trend in the measured V_{oc} at pH 2.9, 5.9, and 8.9, respectively, under 60 mW cm^{-2} of 808 nm illumination for an average of 3−5 runs for each type of electrode. The diffused n^+p junctions displayed nearly identical behavior at all pH values investigated. In contrast, the planar and wire samples that did not contain diffused junctions showed V_{oc} values that strongly depended on pH.[13] The diode quality factor, n, was also calculated for each type of electrode, from the slope of V_{oc} versus the log of the photocurrent density at different illumination intensities (eq 1).

$$V_{oc} = \frac{nk_BT}{q}\ln\left(\frac{J_{ph}}{J_o}\right) \quad (1)$$

where k_B is Boltzmann's constant, T is the absolute temperature, q is the (unsigned) charge of an electron, J_o is the exchange current density, J_{ph} is the photocurrent density, and n is the diode quality factor. Planar p-Si electrodes, and both planar and radial diffused junctions, exhibited n = 1.1−1.2, whereas the diode quality factors for the p-Si wire arrays were 1.5−1.6.

IV. Discussion

All of the electrodes showed rectifying behavior, consistent with a large barrier height at either the Si/liquid or the n^+p Si interface. The measured V_{oc} depends primarily on the band-edge positions of the semiconductor, but also on the kinetics of interfacial electron transfer, carrier generation, and carrier recombination.[23,24] The prominent dependence of V_{oc} on pH, characteristic of p-Si/$MV^{2+/+}$ contacts, was essentially eliminated by the formation of diffused n^+p junctions, which

SCHEME 1: Energy versus Position Diagrams for a p-Type Semiconductor in Contact with a Liquid Electrolyte in the Dark: (a) before Contact, (b) after Contact with a Low-pH Electrolyte, and (c) after Contact with a High-pH Electrolyte[a]

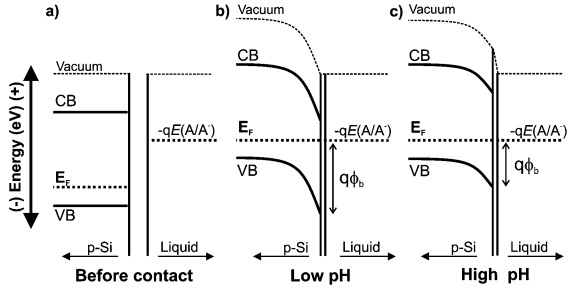

[a] The Fermi level (E_F) of the semiconductor will equilibrate with the solution potential, regardless of where the band positions are located. Because increases in the pH will shift the band edges of Si closer to the vacuum level, for a fixed solution potential, such as that of $MV^{2+/+}$, the barrier height, ϕ_b, will decrease, which decreases the open-circuit voltage under illumination.

SCHEME 2: Energy versus Position Diagrams for an n^+-p-Si Junction in Contact with a Liquid Electrolyte in Equilibrium in the Dark: (a) before Contact, (b) in Contact with a Low-pH Electrolyte, and (c) in Contact with a High-pH Electrolyte[a]

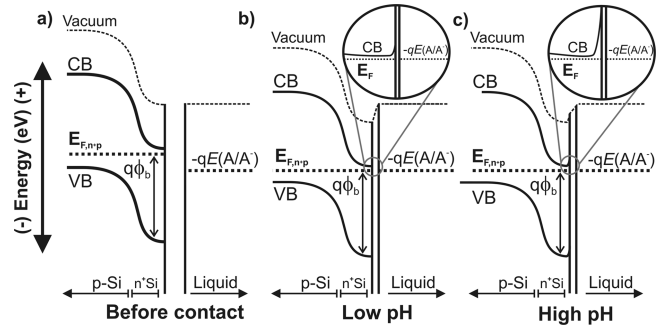

[a] The inset indicates that the surface energetics of the n^+-Si have shifted as in Scheme 1c, except that the high doping of the semiconductor creates a very narrow depletion region, so charge carriers can easily tunnel across the junction. For an n^+-p buried junction, ϕ_b and the open-circuit voltage under illumination are thus decoupled from the pH of the liquid electrolyte.

decoupled the carrier-separating junction from the solid/liquid interface, in both planar and wire array photoelectrodes.

The dependence of V_{oc} on pH for the p-Si (planar and wire array) electrodes can be understood from Scheme 1. Before contact, the bands in the semiconductor are flat (a), but upon contact with the electrolyte, electrons will flow into the semiconductor to equilibrate the Fermi levels across the junction, causing band bending in the semiconductor (b). The barrier height, ϕ_b, i.e., the difference between the valence-band edge of the semiconductor and $qE(A/A^-)$, sets an upper limit on the maximum attainable V_{oc}. The flat band potentials of Si in contact with aqueous electrolytes have been previously reported to vary by -30 mV/pH unit, as revealed by differential capacitance measurements of the semiconductor electrode as a function of pH.[10] This pH dependence is plausibly the result of the acid/base equilibria of surface $-$H and $-$OH groups changing the voltage drop across the double layer at the semiconductor/liquid junction.

At higher pH (Scheme 1c), the shift of the Si band edges toward the vacuum level decreases the barrier height in the system, which should correspond to a decrease in the measured V_{oc}, because $E(MV^{2+/+})$ is independent of pH. The results for both planar p-Si and the p-Si wires support this hypothesis, showing decreased V_{oc} at higher pH. For the planar p-Si samples, V_{oc} shifted by $-(44 \pm 4)$ mV/pH unit, which corresponds well with recent photoelectrochemical measurements of H-terminated p-Si in contact with $MV^{2+/+}$.[13] The open-circuit voltages of p-Si wire array electrodes showed nonlinear behavior with respect to pH, which, along with their higher diode quality factors, suggests the presence of trap states or defects at the wire surface.

The $\Phi_{ext}-E$ data for both the radial and planar n^+p-Si/$MV^{2+/+}$ junctions were nearly identical at all pH values. Electrodes were tested at different pHs over a period of several days, with negligible variation in observed performance. Because the n^+ emitter layer was deliberately not passivated, the band-edge positions of the semiconductor should thus move with pH (Scheme 2). However, the high doping of the emitter gives this contact metallic character, so the band bending occurs across a narrow region of the semiconductor (Scheme 2c inset). On the basis of the surface phosphorus dopant density measured by the spreading resistance ($N_D \sim 10^{19}$ cm^{-3}), the depletion width at the liquid interface should be $\sim$10 nm, which is thin enough that photogenerated carriers can efficiently tunnel across the junction.[25] Hence, the n^+p junction is effectively a floating diode, similar to the GaAs/$GaInP_2$ photocathode device reported by Khaselev and Turner.[26] The invariance in the $J-E$ data relative to a fixed reference potential, across six pH units, provides strong evidence that high photovoltages will be achievable when these wire arrays are decorated with electrocatalysts and used, for example, as photocathodes for solar water-splitting or CO_2 reduction. The Φ_{ext} values of the wire arrays of this particular filling fraction are limited by optical absorption at normal incidence, which can be improved by the introduction of scatterers as well as by other methods.[3−5]

Increasing the attainable photovoltage, and removing the band-edge dependence from Si microwire photocathodes as described herein, could greatly increase conversion efficiency of a hydrogen generating system, which requires a total photovoltage of 1.23 V. Most reports in the literature on p-Si photocathodes for solar water-splitting use noble metal catalysts (Pt, Pd) in acidic electrolytes, but most earth-abundant HER catalysts are not stable at low pH. Hence the ability to operate Si microwire arrays under neutral or alkaline conditions increases the versatility of possible design strategies for use of Si as a water-splitting photocathode. The same principles should apply to buried-junctions in other semiconductors, allowing the creation of devices that decouple the semiconductor energetics from the solution/catalyst interface.

V. Conclusions

In contact with aqueous electrolytes, the introduction of a highly n^+-doped emitter layer not only produced comparable, high photovoltages from planar crystalline p-Si and microwire array p-Si photoelectrodes, but also preserved the high open-circuit photovoltages of such systems over a range of pH values. The invariance of the photoelectrode performance with respect to pH demonstrates that such an approach can decouple the band-edge energetics of the semiconductor from the pH of the solution. High photovoltages can thus be obtained from buried junctions in redox systems that, due to nonoptimal band-edge positions, inherently yield low photovoltages at Si/liquid contacts, such as p-Si/H^+-H_2(aq) contacts, which are limited to photovoltages of $\leq$300 mV regardless of the pH of the electrolyte. The observations thus suggest a route to the

development of efficient buried junction Si microwire photocathodes that can operate efficiently under a wide variety of conditions for fuel-forming reactions, such as photoelectrochemical hydrogen evolution or CO_2 reduction.

Acknowledgment. We acknowledge the Stanford Global Climate and Energy Project and the U.S. Department of Energy (grant DE-FG02-05ER15754) for financial support. We acknowledge critical support and infrastructure provided for this work by the Kavli Nanoscience Institute at Caltech. S.W.B. thanks the Kavli Nanoscience Institute for a postdoctoral fellowship. M.G.W acknowledges support from an NSF American Competitiveness in Chemistry postdoctoral fellowship (CHE-0937048). D. Turner-Evans, J. Ku, and Dr. R. Grimm are thanked for their contributions.

Supporting Information Available: Additional information regarding the VLS growth of Si microwires, photoelectrochemical data correction, and summarized photoelectrochemical performance data are included. This material is available free of charge via the Internet at http://pubs.acs.org.

References and Notes

(1) Bolton, J. R.; Strickler, S. J.; Connolly, J. S. *Nature* **1985**, *316*, 495.

(2) Kayes, B. M.; Atwater, H. A.; Lewis, N. S. *J. Appl. Phys.* **2005**, *97*, 114302.

(3) Boettcher, S. W.; Spurgeon, J. M.; Putnam, M. C.; Warren, E. L.; Turner-Evans, D. B.; Kelzenberg, M. D.; Maiolo, J. R.; Atwater, H. A.; Lewis, N. S. *Science* **2010**, *327*, 185.

(4) Putnam, M. C.; Boettcher, S. W.; Kelzenberg, M. D.; Turner-Evans, D. B.; Spurgeon, J. M.; Warren, E. L.; Briggs, R. M.; Lewis, N. S.; Atwater, H. A. *Energy Environ. Sci.* **2010**, *3*, 1037.

(5) Kelzenberg, M. D.; Boettcher, S. W.; Petykiewicz, J. A.; Turner-Evans, D. B.; Putnam, M. C.; Warren, E. L.; Spurgeon, J. M.; Briggs, R. M.; Lewis, N. S.; Atwater, H. A. *Nat. Mater.* **2010**, *9*, 239.

(6) Plass, K. E.; Filler, M. A.; Spurgeon, J. M.; Kayes, B. M.; Maldonado, S.; Brunschwig, B. S.; Atwater, H. A.; Lewis, N. S. *Adv. Mater.* **2009**, *21*, 325.

(7) Warren, E. L.; Boettcher, S. W.; McKone, J. R.; Lewis, N. S. In *Proceedings of SPIE 7770*; Idriss, H., Wang, H., Eds.; SPIE: Bellingham, WA, 2010; Vol. 7770, p 77701F. DOI: http://dx.doi.org/10.1117/12.860994.

(8) Dominey, R. N.; Lewis, N. S.; Bruce, J. A.; Bookbinder, D. C.; Wrighton, M. S. *J. Am. Chem. Soc.* **1982**, *104*, 467.

(9) Lewis, N. S. *J. Electrochem. Soc.* **1984**, *131*, 2496.

(10) Madou, M. J.; Loo, B. H.; Frese, K. W.; Morrison, S. R. *Surf. Sci.* **1981**, *108*, 135.

(11) Hamann, T. W.; Lewis, N. S. *J. Phys. Chem. B* **2006**, *110*, 22291.

(12) Hunger, R.; Fritsche, R.; Jaeckel, B.; Webb, L. J.; Jaegermann, W.; Lewis, N. S. *Surf. Sci.* **2007**, *601*, 2896.

(13) Johansson, E.; Boettcher, S. W.; O'Leary, L. E.; Polatayev, A.; Lewis, N. S. *J. Phys. Chem.* Submitted for publication.

(14) Nakato, Y.; Egi, Y.; Hiramoto, M.; Tsubomura, H. *J. Phys. Chem.* **1984**, *88*, 4218.

(15) Johnson, E. L. *Technical Digest -International Electron Devices Meeting*; IEEE: New York, 1981; p 1. DOI: 10.1109IEDM.1981.189984.

(16) Kayes, B. M.; Filler, M. A.; Putnam, M. C.; Kelzenberg, M. D.; Lewis, N. S.; Atwater, H. A. *Appl. Phys. Lett.* **2007**, *91*, 103110.

(17) Kelzenberg, M. D.; Turner-Evans, D. B.; Kayes, B. M.; Filler, M. A.; Putnam, M. C.; Lewis, N. S.; Atwater, H. A. *Nano Lett.* **2008**, *8*, 710.

(18) Putnam, M. C.; Turner-Evans, D. B.; Kelzenberg, M. D.; Boettcher, S. W.; Lewis, N. S.; Atwater, H. A. *Appl. Phys. Lett.* **2009**, *95*, 163116.

(19) Fahrenbruch, A. L.; Bube, R. H. *Fundamentals of Solar Cells*; Academic Press: New York, 1983.

(20) Spreading resistance measurements were performed by Solecon Laboratories Inc.

(21) The Φ_{ext}, electrons collected per incident photon, is directly proportional to the observed photocurrent density (see Supporting Information).

(22) Bocarsly, A. B.; Bookbinder, D. C.; Dominey, R. N.; Lewis, N. S.; Wrighton, M. S. *J. Am. Chem. Soc.* **1980**, *102*, 3683.

(23) Hamann, T. W.; Gstrein, F.; Brunschwig, B. S.; Lewis, N. S. *J. Am. Chem. Soc.* **2005**, *127*, 13949.

(24) Hamann, T. W.; Gstrein, F.; Brunschwig, B. S.; Lewis, N. S. *Chem. Phys.* **2006**, *326*, 15.

(25) Sze, S. M.; Ng, K. K. *Physics of Semiconductor Devices*; Wiley-Interscience: New York, 2006.

(26) Khaselev, O.; Turner, J. A. *Science* **1998**, *280*, 425.

JP109147P